

**Stator winding fault diagnosis of Induction Motor using FFT**S.M.Shashidhara  
Professor

Dept of EEE, RYM Engineering College, Ballari, India

---

**Abstract**— In this paper, FFT and its implementation with problem of fault detection in the stator windings of induction motor has been presented. The Fourier transform converts the time domain into equivalent frequency domain or vice versa. FFT is the potential and highly efficient approach for performing aforementioned conversion by factorization of DFT matrix into a product of sparse factors. This efficiency makes FFT applicable for fault detection approaches in motors using motor current signature analysis (MCSA). FFT based spectrum analysis has been presented for healthy as well as faulty motor.

---

**Keywords**— Fast Fourier Transform, Induction Motor, Stator winding Fault, MCSA, Fault frequency components

**I. INTRODUCTION**

There is a consensus among researchers that 35-40 % of induction motor breakdowns are associated with the stator winding insulation [1]. Further, it is generally assumed that important parts of stator winding-related failures are initiated by insulation failures in numerous turns of a stator winding within one phase. This type of fault is familiar as a 'turn fault' [2]. A stator turn fault in an alternating current machine sets off the flow of elevated circulating current and therefore, produces excessive heat in the shorted turns. If the heat proportionate with the square of the circulating current goes beyond the constraining magnitude, it may result in the failure of the motor.[3]. Nevertheless, the worst outcome of a stator turn fault may be a grave accident resulting in loss of life. The organic materials employed for insulation in electric machines are prone to considerable deterioration from a coalition of factors viz., thermal overloading and cycling, stresses due to transient voltage on the insulation material and mechanical stresses.

Among the likely causes, thermal stresses are primarily responsible for the degradation of the stator winding insulation. Thermal stresses effecting stator winding insulation failure are classified into three categories: aging, overloading, and cycling [4]. Even the superior insulation may fall short if motor is run beyond its temperature upper limit. As a convention, the life span of the insulation is lessened by 50% for every 10°C raise over the stator winding temperature limit [5]. Therefore, it is needed to check the stator winding temperature so that a machine will not operate past its thermal range. For this reason, several methods have been put forward [6,7].

The current in the stator winding results in a force on the coils that is proportional to the square of the current. This force is at its greatest under transient overloads, resulting in the coils to pulsate at twice the synchronous frequency with shifting in both the radial and the tangential direction. This movement deteriorates the reliability of the insulation system. Mechanical faults, such as damaged rotor bar, worn bearings, and air gap eccentricity, may be a cause why the rotor hits the stator windings. Hence, such mechanical failures should be identified before they breakdown the stator winding insulation [6,7].

Contamination due to unknown materials can result in undesirable outcomes on the stator winding insulation. The presence of strange and foreign contaminants can cause a decline in heat dissipation [8]. It is therefore, of utmost importance to keep the motors dirt free and dry, in particular, when the motors run in a hostile environment. Despite the causes, stator winding-related breakdown can be segregated into five types: turn-to-turn, coil-to-coil, line-to-ground, line-to-line, and open circuit faults. Among the five failure modes, turn-to-turn fault (stator turn fault) is supposedly the most challenging one since the other forms of breakdowns are generally the result of turn faults [9,10]. In addition, turn faults are very arduous to identify at their primitive stage. To crack the difficulty in identifying turn faults, many techniques have been devised [11,12]. In this research work, stator short winding fault has been diagnosed using the Park's vector, spectrum analysis and DWT based approaches.

Fig. 1 illustrates the stator winding faults in induction motor. In Fig. 2, photos in upper section, show a healthy winding status, while the photos shown in lower section, exhibit the faults caused due to winding irregularity and burn outs.

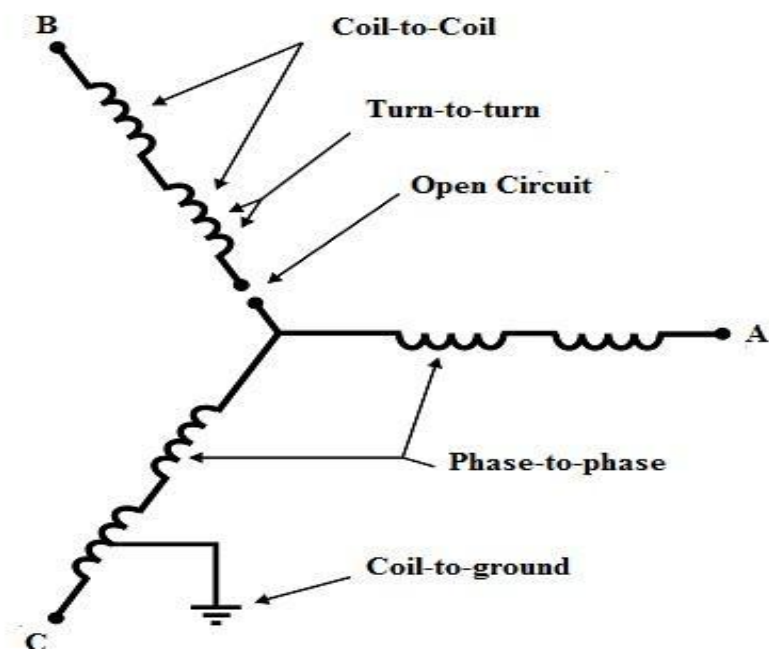


Fig. 1 Stator winding faults of Induction Motor

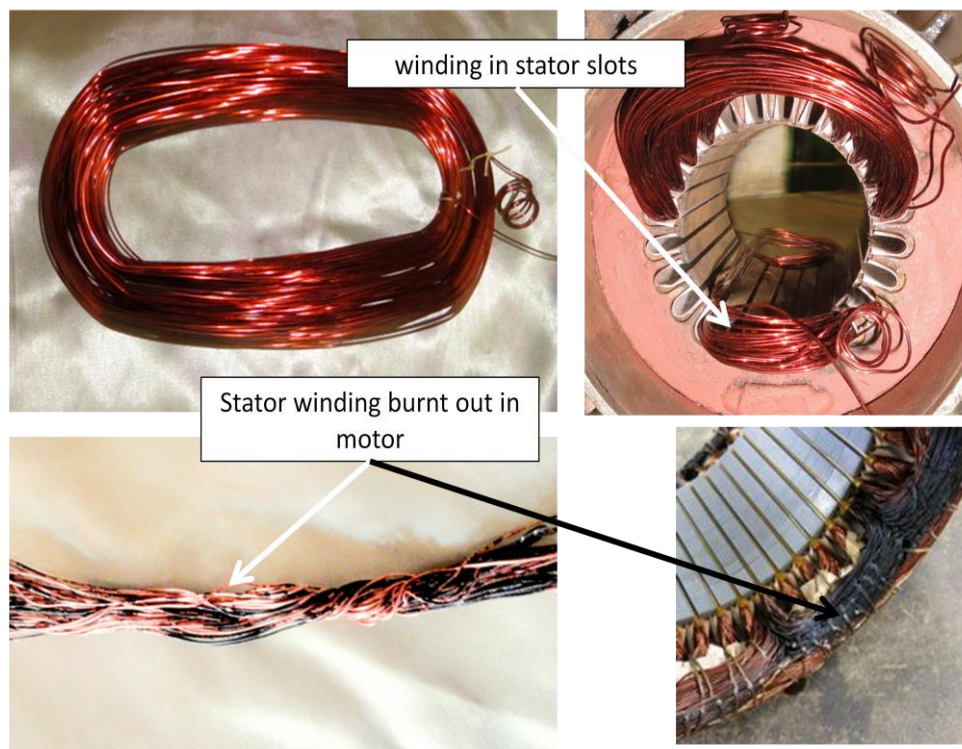


Fig. 2 Stator winding coils

Such faults of winding irregularity, and their effect on induction motor function, have been investigated experimentally in this study. Stator windings were shorted artificially to emulate the fault condition.

## II. EXPERIMENTAL SETUP

The diagnosis of shorted turns in stator windings of an induction motor, using MCSA, is based on detecting the frequency components given by following equation [13,14].

$$f_{st} = f_s \left[ \frac{(1-s)}{p} \right] \quad (1)$$

The experimental setup has been shown in Fig. 3. The 3-phase induction motor being implemented is having parameters: 415V, 1 HP,  $f=50\text{Hz}$ , 1440 rpm, 2 pole pairs.

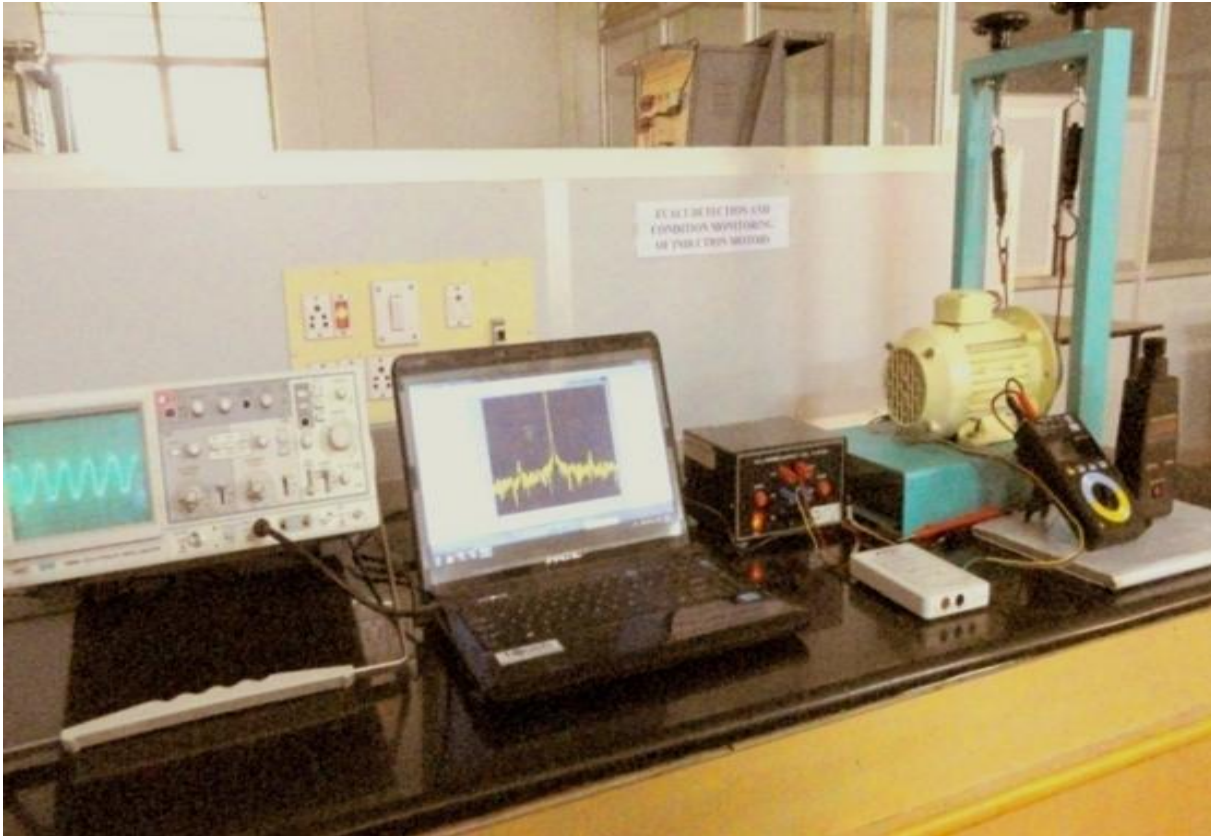


Fig. 3 Experimental setup

The measurement and its analysis can be performed with multiple operational devices, and the acquired data can be fetched with the help of a robust software tool LabVIEW™. In order to obtain the sample current value in, the data acquisition card myDAQ was employed that obtains the value from the motor under load.

NI myDAQ is a data acquisition (DAQ) device that gives the ability to measure and analyse live signals. myDAQ includes two analog inputs and two analog outputs at 200 kS/s and 16 bits, allowing for applications such as sampling a sensor output signal; eight digital inputs and output lines.

Flow diagram of fault diagnosis is shown in Fig. 4. In this work, speed was computed by using the tachometer. The virtual instrument (VI) panel (Fig. 5) was developed while employing the algorithms developed in LabVIEW. The VI was functional for the purpose of measurement as well as the processing along with continuous data acquisition. For assessing the system while considering the practical conditions, frequent measurements were carried out to get the stator current of the motor.

The VI data acquisition block needs the number of samples, scan rate frequency resolution and channel information to be specified. Power spectrum subVI performs FFT analysis of the stator current signal. Spectrum graph is displayed on the front panel of the software. A time window of 175 ms was used for all data acquisitions for accomplishing a straightforward and comprehensive pattern. Power spectrum program of LabVIEW advanced signal processing software was used for the analysis.

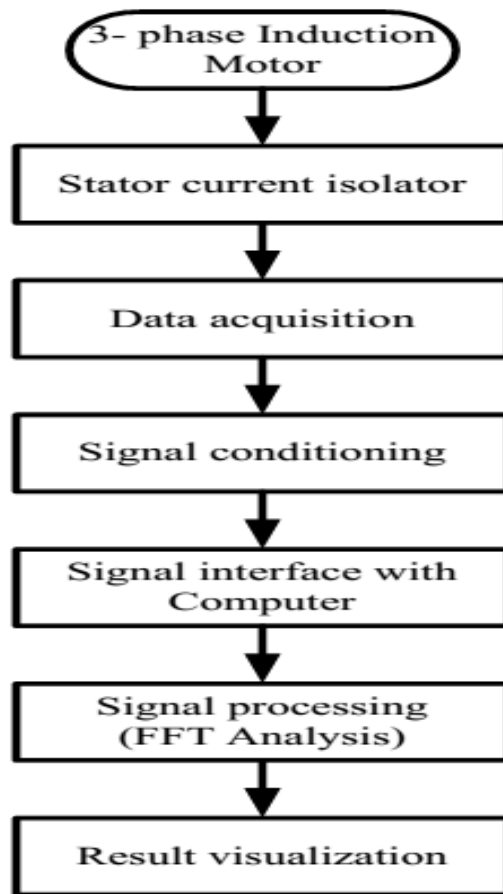


Fig. 4 Flow diagram of Fault diagnosis

### III. ANALYSIS OF STATOR TURN-TO-TURN FAULTS

Experiments were conducted in the laboratory, first on a healthy motor, followed by faulty motor and results are demonstrated. The equation for fault frequency components due to stator short circuit fault is given by following equation.

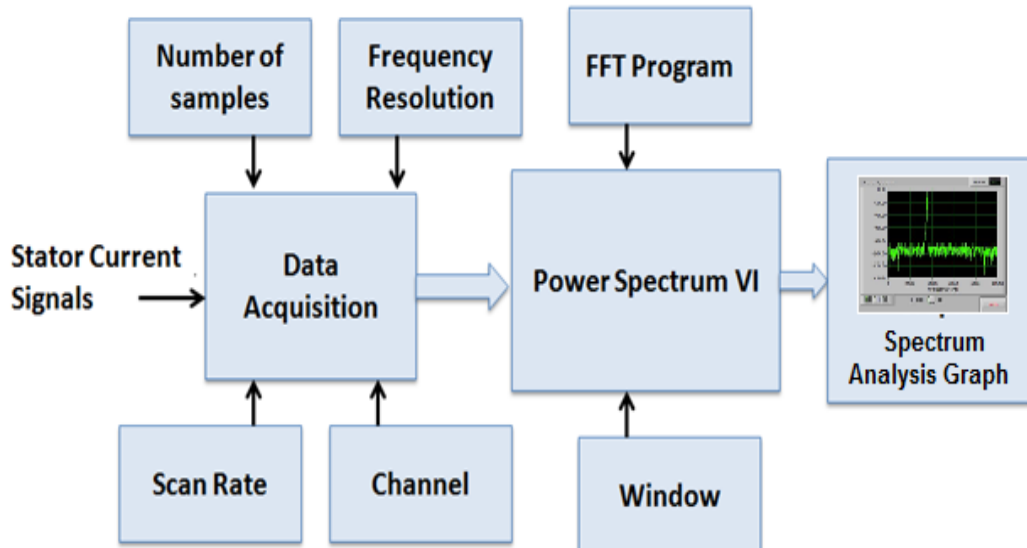


Fig. 5 Block diagram of the Virtual Instrument Panel

$$f_{st} = f_s \cdot k \left[ \frac{n}{p} (1 - s) \right] \tag{2}$$

Where,  $f_{st}$  is the frequency component due to turn-to-turn fault in the stator winding.  $f_s$  denotes supply frequency while ‘ $p$ ’ is the number of pole pairs, ‘ $s$ ’ denotes slip speed,  $n$  and  $k$  are the natural numbers [13].

When  $k = 1$ , the component frequency, induced in the spectrum of the stator current, superimposed on the fundamental current, will be illustrated by the following formula

$$f_{st} = f_s \left[ \frac{n}{p} (1 - s) \right] \tag{3}$$

For four pole motors ( $p = 2$ ), the equation will be revealed in the following series of components:

$$f_{st} = \begin{cases} \left(\frac{1}{2}\right) f_s (1 - s) & n = 1 \\ f_s (1 - s) & n = 2 \\ \left(\frac{3}{2}\right) f_s (1 - s) & n = 3 \end{cases} \tag{4}$$

These components are visible in the frequency spectrum of the stator current, as sidebands to the fundamental peak. It can be used as a good indicator of the stator short circuit fault. However, putting  $n = 1$  in following equation, we can get

$$f_{st} = f_s \left[ \frac{(1-s)}{p} \right] \tag{5}$$

The above-mentioned equation expresses the relationship between the fault frequency component and slip.

The Table 1 and the corresponding Fig. 6 demonstrate the variation of the motor slip value for different turn-to-turn short circuits. The slip value rises while the load level increases. At the same load level, the slip value for 20% turns fault is smaller than the value of 5% short turn fault.

TABLE 1  
 SLIP VALUE VARIATION WITH LOAD AND STATOR WINDING FAULT

Load	5% short	10% short	20% short
NL	1.44	1.3	1.2
HL	3.9	3.5	3.1
FL	5.5	5.1	4.8

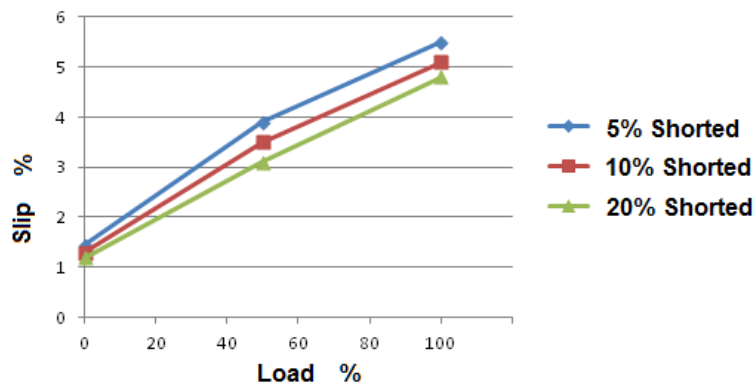


Fig. 6 Slip value vs. load and stator winding fault

In this section, the frequency components in the current signal, when  $n = 1$ ,  $p = 2$  and  $k = 1$  in equation (2), are investigated and analyzed. In addition, three sets of turn-to-turn faults are tested with 5% turns short circuit, 10% turns short circuit and 15% turns short circuit[13].

Here, Typical calculations of fault frequencies is shown for a case; when a healthy motor is at 80% load, the measured rotor speed is 1471 rpm. Therefore, the slip,  $s=(1500-1471)/1500\approx 0.0186$ , and the fault component frequency can be computed as,

$$f_{st} = 1/2 \times 50 \times (1 - s) \approx 24.53 \text{ Hz.} \tag{6}$$

When  $k = 1$ , according to equation (2), the fault frequency is

$$f_{st} = |24.5 \pm 50| \text{ Hz.} \tag{7}$$

Thus, the left and right side band fault frequencies on the frequency spectrum are

$$f_{st0} = |24.53 - 50| = 25.46 \text{ Hz and} \tag{8}$$

$$f_{st1} = |24.53 + 50| = 74.53 \text{ Hz, respectively.} \tag{9}$$

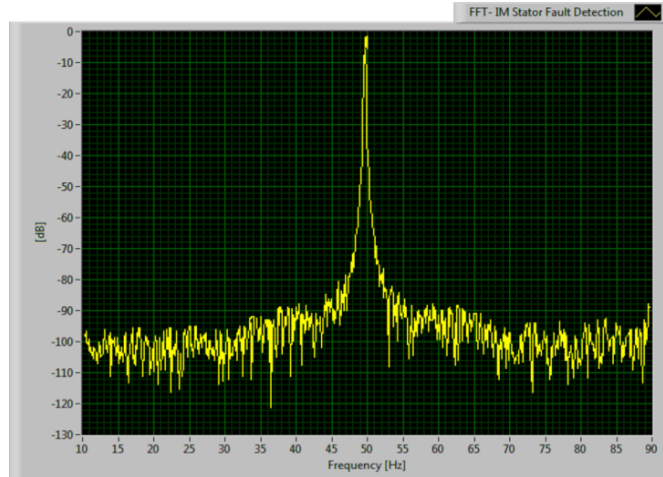


Fig. 7 FFT of stator current of healthy Motor at No-Load

Fig. 7 demonstrates the frequency spectrum of the stator current data at no-load. In this Fig., the fault frequencies are not found in the side band, as the motor stator windings are healthy. While the healthy motor operates at 100% load level, as the motor is healthy, fault frequencies are not observed in the frequency spectrum. This is demonstrated in Fig. 8.

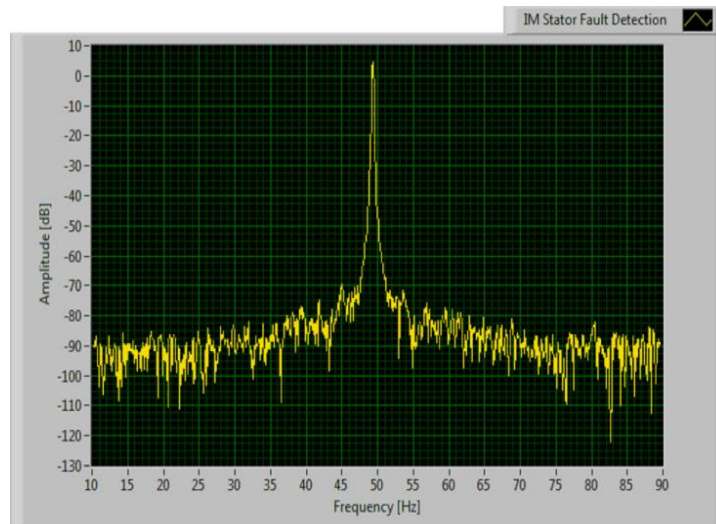


Fig. 8 FFT of stator current of healthy motor at Full-load

When a turn-to-turn fault happens, the variations in the current signal are depicted in Fig. 9. They are the test results for 5% turns short circuit. Although there is a slight difference with the frequencies computed and experimentally plotted on graph, the error is within tolerance because the difference is produced by the noise of the load level. The magnitude at fault frequency 25.36 Hz increases to -90dB. Therefore, we can conclude that when the motor operates with a turn-to-turn fault, the amplitude of specific fault frequencies will increase, as expected. The test results for 5%, 10% and 20% short circuit fault of stator winding are presented in Tables 2, 3 and 4 respectively.

A. Stator windings shorted at 5%

TABLE 2

VARIATIONS OF FAULT FREQUENCY COMPONENTS AND THEIR MAGNITUDES  
 WITH LOAD AT 5% STATOR WINDING FAULT

	Load	Slip (pu)	LSB (Hz)	Magnitude (dB)	USB (Hz)	Magnitude (dB)
NL	0	1.44	25.36	-90	74.64	-90
HL	50	3.9	25.98	-88	74.03	-88
FL	100	5.5	26.38	-86	73.63	-86

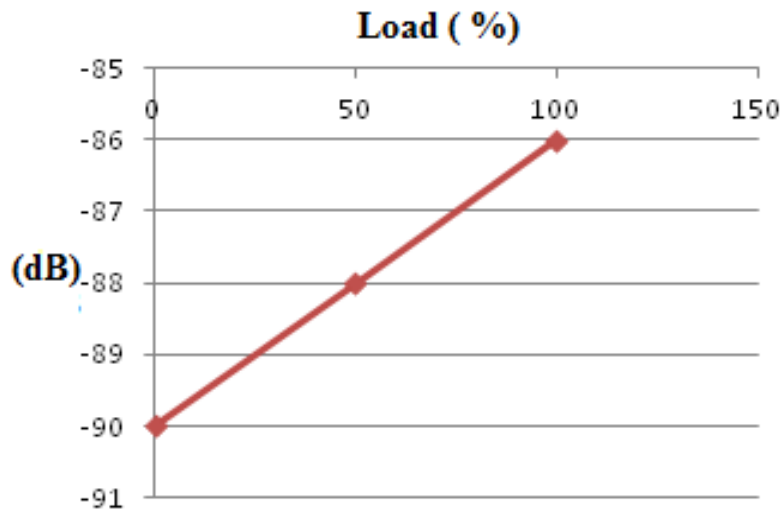


Fig. 9 Variations of magnitudes of fault frequency components in dB with load at 5% stator winding fault

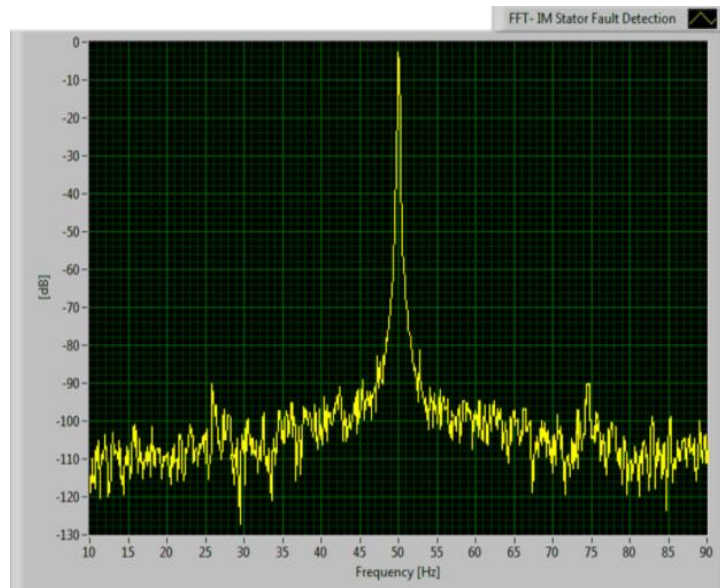


Fig. 10 FFT of stator current at 5% Short circuit No-Load

**B. Stator windings shorted at 10%**

TABLE 3  
 VARIATIONS OF FAULT FREQUENCY COMPONENTS AND THEIR MAGNITUDES  
 WITH LOAD AT 10% STATOR WINDING FAULT

	Load	Slip (pu)	LSB (Hz)	Magnitude (dB)	USB (Hz)	Magnitude (dB)
NL	0	1.3	25.33	-87	74.68	-87
HL	50	3.5	25.88	-84	74.13	-84
FL	100	5.1	26.28	-82	73.73	-82

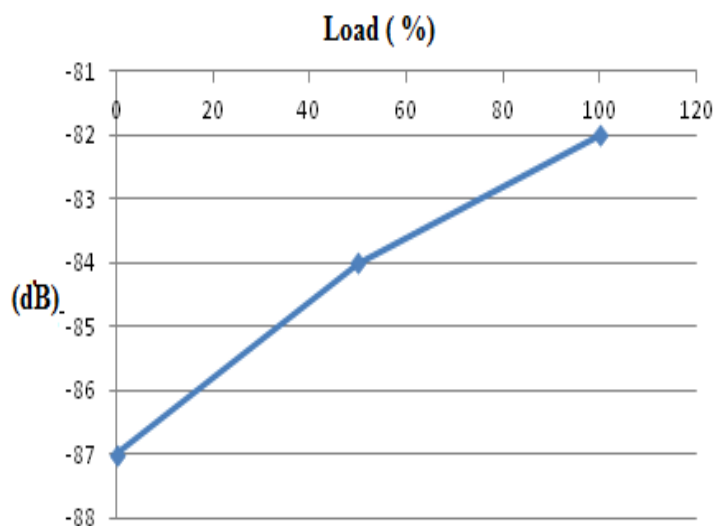


Fig. 11 Variation of magnitudes of fault frequency components in dB with load at 10% stator winding fault

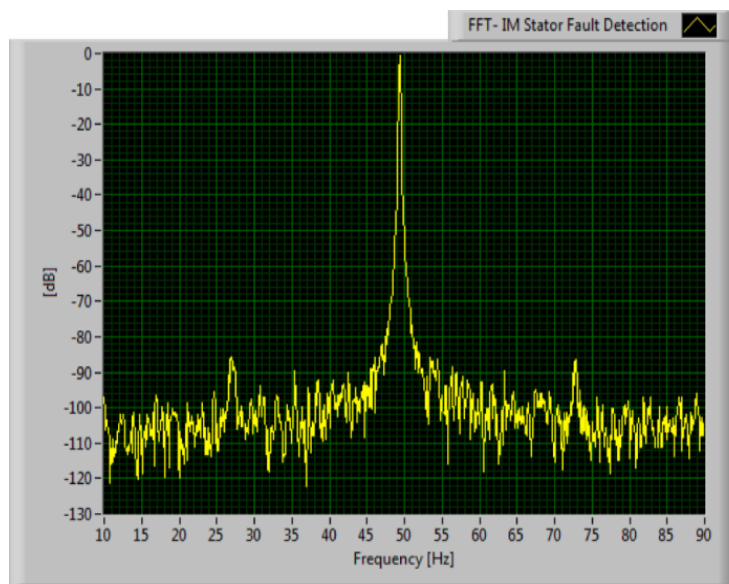


Fig. 12 FFT of stator current at 10% Short circuit Full-Load

**C. Stator windings shorted at 20%**

TABLE 4

VARIATION OF FAULT FREQUENCY COMPONENTS AND THEIR MAGNITUDES  
 WITH LOAD AT 20% STATOR WINDING FAULT

	Load	Slip (pu)	LSB (Hz)	Magnitude (dB)	USB (Hz)	Magnitude (dB)
NL	0	1.2	25.30	-80	74.70	-80
HL	50	3.1	25.78	-76	74.23	-76
FL	100	4.8	26.20	-72	73.80	-72

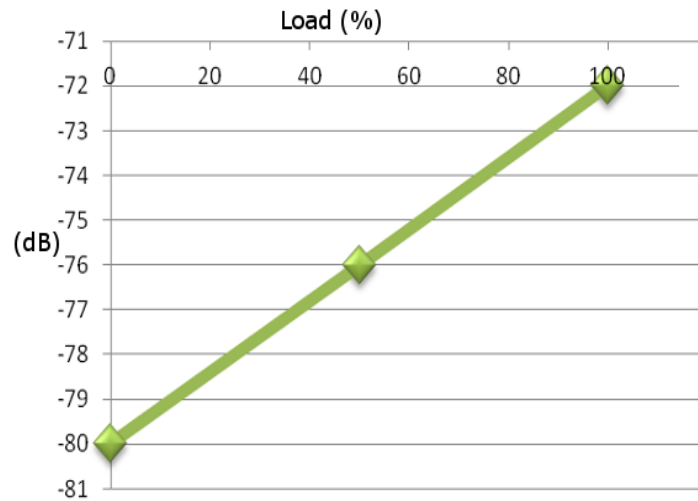


Fig. 13 Variations of magnitudes of fault frequency components in dB with load at 20% stator winding fault

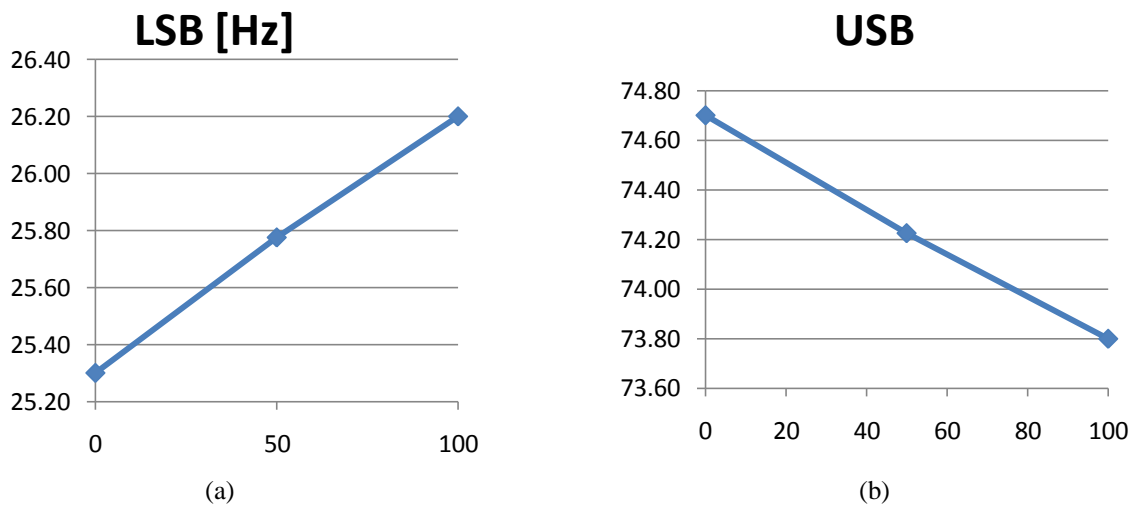


Fig. 14 Fault Frequency variation with load at 20% shorted windings:  
 (a) in Lower Side Band (b) in Upper Side Band

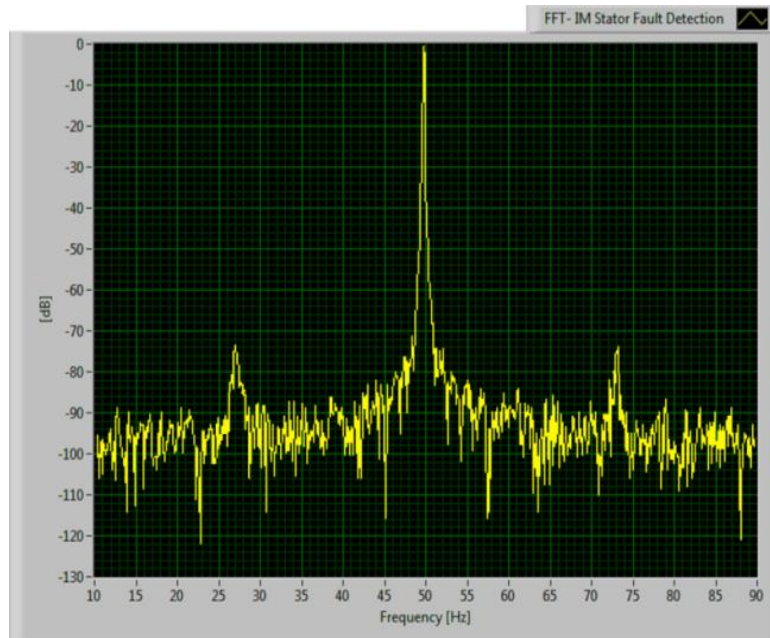


Fig. 15 FFT of stator current at Full-load and 20% turns shorted

#### IV CONCLUSIONS

In each test, the harmonic frequencies and the corresponding amplitudes are recorded at different loading conditions. In addition, the slip values are computed and the variations in fault frequency amplitudes are plotted for different load levels. It may be observed from the results that, the magnitude of the fault frequency is a function of the load level. At higher load levels, the fault frequency components are prominently visible; whereas at low loads, they are less noticeable.

Motor current Signature Analysis using FFT needs only one stator current and non-invasive. This is a simple and also an accurate method. Harmonics in the stator current of the motor are studied in this method. These harmonics are produced by new revolving flux components due to a fault. This study needs only one current sensor and is based on FFT. This methodology and the results provide reliable results. It is possible from this technique to detect the fault and to evaluate its severity.

#### REFERENCES

- [1] IAS MR Working Group, "Report of large motor reliability survey of industrial and commercial installation, *IEEE Trans. Industry Applications*, vol. I-A-21, pp. 853-864, Jul/Aug, 1985.
- [2] Sottile Jr, Joseph, and Jeffery L. Kohler. "An on-line method to detect incipient failure of turn insulation in random-wound motors." *Energy Conversion, IEEE Transactions on* 8, no. 4, 762-768, 1993.
- [3] S.B.Lee, R. M. Tallam, and T. G. Habetler, "A robust, on-line turn fault detection technique for induction machines based on monitoring the sequence component impedance matrix," *IEEE Transactions on Power Electronics*, vol. 18, no.3, pp. 865-872, May, 2003.
- [4] A. H. Bonnet and G. C. Soukup, "Cause and analysis of stator and rotor failures in three- phase squirrel case induction motors," *IEEE Trans. Industry Application*, vol., 28, no. 4, pp.921-937, 1992.
- [5] T. A.Lipo, *Introduction of AC machine design*, Wisconsin Power Electronics Research Center, 2nd edition, 2004.
- [6] S. F. Farag, R. G. Bartheld, and W. E. May, "Electronically enhanced low voltage motor protection and control," *IEEE Trans. Industry Applications*, vol. 29, no.1, pp. 45-51, 1994.
- [7] S.B.Lee and T.G.Habetler, "An on-line stator winding resistance estimation technique for temperature monitoring of line-connected induction machines," *IEEE Trans. Industry Applications*, vol. 39, no.3, pp. 685-694, May/June, 2003.
- [8] WL Roux, RG Harley, and TG Habetler, "Detecting rotor faults in permanent magnet synchronous machines," in *Conf. Rec. SDEMPED 03*, Atlanta, GA, USA, pp. 198-203, August, 2003.
- [9] J.R.Stack, T. G. Habetler, and R. G. Harley, "Bearing fault detection via autoregressive stator current modeling," *IEEE Trans. Industry Applications*, vol. 40, no.3, pp. 740-747, May/June, 2004.
- [10] M.A.Cash, "Detection of turn faults arising from insulation failure in the stator windings of AC machines," *Doctoral Dissertation*, Dept. of Electrical and Computer Engineering, Georgia Institute of Technology, USA, 1998.

- [11] D.E.Schump, "Predict motor failure with insulation testing," *Pulp and Paper Industry Tech Conference 1997*, pp.48-50, Cincinnati, OH, USA, Jun, 1997.
- [12] R. Maier, "Protection of squirrel-cage induction motor utilizing instantaneous power and phase information," *IEEE Trans. Industry Applications*, vol. 28, pp. 376-380, 1992.
- [13] S.M.Shashidhara and Dr.P.Sangameswara Raju; "Fault Detection of Three-Phase Induction Motor based on Motor Current Signature Analysis" in *International Conference on Convergence of Science, Engineering and Management (ICCSEM-2013)* held at Dayanand Sagar College of Engineering, Bangalore on 26-27 Sept 2013.
- [14] S.M.Shashidhara and Dr.P.Sangameswara Raju; "Diagnosis Of Broken Rotor Bars in Induction Motor by using Virtual Instruments" Published in *International Journal Of Electrical Engineering and Technology (IJEET)*, ISSN Print: ISSN 0976-6545 ISSN, Online: ISSN 0976-6553, Vol. 4, Issue 5, September – October 2013, pp. 78-86.